Desalination 344 (2014) 252–265

Contents lists available at ScienceDirect

Desalination

journal homepage: www.elsevier.com/locate/desal

Structural optimization of seawater desalination: I. A flexible superstructure and novel MED–MSF configurations

Tawfiq H. Dahdah [a], Alexander Mitsos [a,b,*]

[a] Department of Mechanical Engineering, Massachusetts Institute of Technology, 77 Massachusetts Avenue, Cambridge, MA 02139, USA
[b] AVT Process Systems Engineering (SVT), RWTH Aachen University, Turmstrasse 46, Aachen 52064, Germany

HIGHLIGHTS

- We structurally optimize thermal desalination systems.
- We develop a superstructure representing existing and novel thermal desalination structures.
- The superstructure is optimized without binary variables using BARON.
- Optimization of feed routing results in substantial improvements.
- New desalination structures are identified.

ARTICLE INFO

Article history:
Received 18 December 2013
Received in revised form 17 March 2014
Accepted 19 March 2014
Available online 18 April 2014

Keywords:
Desalination
Superstructure
Hybrid thermal desalination systems
Multi-objective optimization
MED
MSF

ABSTRACT

A methodology is proposed to identify improved thermal-based desalination structures. It is based on the notion of superstructure, allowing for the simultaneous representation of numerous feed, brine and vapor routing schemes. By adjusting the flow routings, the superstructure is capable of representing the common thermal desalination structures, as well as an extremely large number of alternate structures, some of which might exhibit advantageous behavior. The superstructure is built around a repeating unit which is a generalization of an effect in a multi-effect distillation system (MED) and a stage in a multi-stage flash system (MSF). The superstructure is proposed as an improved tool for the structural optimization of thermal desalination systems, whereby the optimal selection of components making up the final system, the optimal routing of the vapors as well as the optimal operating conditions are all variables simultaneously determined during the optimization problem. The proposed methodology is applicable to both stand-alone desalination plants and dual purpose (water and power) plants wherein the heat source to the desalination plant is fixed. It can be extended to also consider hybrid thermal–mechanical desalination structures, as well as dual purpose plants where the interface of power cycle and desalination is also optimized for.

1. Introduction

1.1. Pressing need for desalination

The global demand for a steady, economical supply of fresh water continues to increase. One of the main known modes of increasing the existing water supply is seawater desalination; a proven process that can reliably convert the seemingly limitless supply of seawater to high-quality water suitable for human consumption. Already, desalination plants operate in more than 120 countries in the world, including Saudi Arabia, the United Arab Emirates, Spain, Greece and Australia. While large-scale desalination plants have been available for a long time, further installations are expected to increase at an alarmingly fast rate, with most of the desalination plant installations expected to be of either the thermal or membrane type. It is projected that by just 2016, the global water production by desalination will increase by more than 60% from its value in 2010 [1]. In Gulf countries in specific, where energy costs are low and where the high salinity waters complicate the use of membrane-based technologies, thermal desalination technologies are foreseen to continue to dominate the market in the nearby future. Thus, the need to enhance thermal desalination technologies, which include the multi-effect distillation (MED) and multi-stage flash distillation (MSF) plants, continues to be a pressing issue. It has already been tackled by many authors, and will be addressed in the work presented herein.

Seeking to contribute improvements to this field, authors have undertaken varying approaches. Several authors, through parametric

* Corresponding author at: Department of Mechanical Engineering, Massachusetts Institute of Technology, 77 Massachusetts Avenue, Cambridge, MA 02139, USA.
E-mail address: amitsos@alum.mit.edu (A. Mitsos).

http://dx.doi.org/10.1016/j.desal.2014.03.030

studies, investigated the influence of numerous variables to gauge their relative importance on performance of MED plants [2–6]. These variables include the total number of effects, the temperature and salinity of the incoming feed, the temperature of the heating steam, as well as the temperature of the evaporator in the last effect. While such studies occasionally provide useful insights, most of the relationships that arise, e.g., distillate production is heavily dependent on the number of effects, are mostly expected. Moreover, the results of such studies are of limited use to designers, mainly because parametric studies do not consider interaction between the different system variables. The need for optimization is clear.

To optimize thermal desalination plants, authors have resorted to differing objective functions. In certain situations, the objective functions are economic related such as minimizing unit product cost or minimizing specific heat transfer areas. In others, the objectives are tied to the thermodynamics such as maximizing distillate production or exergy efficiency [7–9]. While single objective functions are frequently resorted to, multi-objective optimizations are generally preferable. The main reason is that single objective optimization does not necessarily yield applicable designs. For instance, if the distillate production is maximized as part of a single objective study, the associated costs are not directly considered. The result is generally an uneconomical unimplementable plant. In contrast, multi-objective optimization studies can consider both efficiency and economic measures, resulting in more realistic designs. Further, multi-objective optimization allows the quantification of the trade-offs between competing criteria.

The works directed to improve thermal desalination have taken numerous fronts. Some authors have considered the stand-alone optimization of thermal-based configurations. While some of these authors optimized operating conditions associated with pre-existing configurations, others proposed alternative schemes – such as the MSF–MED proposed in [10,11] – which they subsequently optimized and compared to conventional structures. Other authors meanwhile have examined hybrid thermal-membrane based technologies seeking to make use of the ease of their integration. By suggesting alternative flow routing possibilities, authors propose that the resulting hybridized structures offer significant synergetic benefits. These advantages include, but are not restricted to, the reduction of capital costs through use of common intake and outfall facilities, the potential for reduced pretreatment and an increase in top brine temperature in thermal desalination [12–18]. Other authors propose integrating thermal desalination configurations with thermal vapor compression systems as an efficient means of increasing total distillate production, reducing cooling water requirements and potentially reducing heat transfer area requirements, all while being characterized by simple operation and maintenance [19,20].

While the aforementioned contributions have resulted in more efficient desalination plants with improved economics, one significant drawback impedes even larger improvements. The general practice of fixing both the hardware, i.e., technology choice such as MED or MSF, involved in a plant, as well as its flowsheet prior to optimization, results in more tractable optimization problems but has obvious shortcomings. It can be easily seen that an alternate optimization approach whereby both the hardware and the flowsheet could be modified during the optimization process is preferable. This is especially true since there is no guarantee that any of the common configurations already proposed in literature is optimal under any conditions. For studies concerning hybrid plants in particular, the more flexible optimization could yield breakthroughs as there might be significant benefit from deviating from the conventional setups specific to stand-alone structures. Herein, a methodology for simultaneous optimization of flowsheet and design/operation using the notion of superstructure is utilized [21]. The superstructure is composed of a series of units, allowing for vapor formation by two processes. One option is evaporation of brine within an effect, and subsequent condensation of the produced vapor in a feed preheater or a subsequent effect; this is in essence an MED stage. An alternate mode of vapor formation involves the flashing of brine entering into a flash box, and condensation in a preheater, or in a subsequent effect; this is similar to the MSF process.

The general need to investigate modifications in hardware and flow patterns has been looked into. Authors generally proceed to propose a series of modifications they envision to be advantageous. They subsequently optimize the resulting arrangements, and compare the results to those exhibited by conventional structures to decide on the merit-worthiness of their ideas. Unfortunately, such a series of steps is time consuming and their success in yielding improved results depends highly on both the author's experience and creativity. This method is further restrictive because the testing of the huge number of combinations of different possible flowsheets and hardware is infeasible.

Note that herein, desalination-only plants are assumed. However, by design the methodology can be easily extended to a number of alternate applications, including optimizing cogeneration hybrid facilities. This is achievable since the model of the superstructure tool proposed can easily be integrated with the model of a power plant. One way to optimize a dual-purpose plant is to keep the interface between the power cycle and the desalination unit fixed and optimize each on its own. The case study presented in our manuscript is in that way directly applicable. The only element missing would be to optimize the interface, which is in essence the flow rate and temperature of the steam taken from the power cycle (extraction or back-pressure) used as a heat source for the desalination.

2. Superstructure concept for optimizing thermal desalination structures

Herein, we propose a flexible methodology that is capable of adjusting the process diagram of thermal desalination configurations. It is based on the concept of a superstructure, and is able to adjust the hardware component set, the routing of all the different flows entering and exiting each of the eventual components making up the system, as well as adjusting the sizing of all the necessary components. Through this process, all the existing thermal desalination configurations can be represented, in addition to an extremely large number of alternative configurations, making it ideal for the systematic comparison of alternatives and the generation of new ones. Note that the superstructure is a notion employed in process design that illustrates all the different hardware and connectivity possibilities to be considered for optimal process design [21].

The methodology allows for improved optimization studies involving thermal configurations. Further, it can be easily adjusted to be used in optimization studies of hybrid configurations involving membrane-based technologies and thermal vapor compression systems, considered in the second part of the article. The tool can be modified to investigate co-generation by integrating it with a power plant model. To illustrate the usefulness of the proposed methodology, the results of several multi-objective optimization studies are presented, whereby the performance improvements are quantified, while the optimal flow patterns are shown to deviate from the convention.

While the origin of the superstructure approach is in the chemical process industry, authors have recently utilized it in the field of desalination. Zak [22], by identifying physical processes shared by all thermal desalination technologies, constructed a superstructure capable of representing existing thermal desalination configurations as well as novel ones, however did not optimize it. Sassi and Mujtaba [23] used it to identify optimal RO networks for a variety of differing temperatures and salinities. The study confirmed, as expected, that such factors have a significant impact on the subsequent optimal design and operation. Skiborowski et al. [24], on the other hand, optimized a superstructure considering the combination of an RO network with an MED configuration specified to be of the forward feed type. Again, the work demonstrates that optimal configuration varies depending on local factors such as the energy costs and pretreatment costs. As a final example, Mussati et al. [25–27] used a superstructure for varying purposes including identifying optimal coupling of power and desalting plants and identifying improvements in the design of MSF plants.

3. Description of conventional thermal desalination processes

The process of constructing a general superstructure to represent thermal desalination structures is greatly facilitated by the fact that both MED and MSF operate on the same fundamental principles. Both processes require an external heat input to drive the initial production of vapor, and an external work input to drive the pumps which are needed to overcome the different pressure losses experienced by the flows.

In MED, the external heat input is used to first sensibly heat the incoming feed to the first effect and subsequently evaporate a portion of it. Two separate streams consequently exit the effect: a more concentrated brine stream, and a saturated vapor stream. The saturated vapor is split; a portion of it is used to pre-heat the feed in a counter-current feed preheater while the remaining portion is used as heating steam to the next effect where additional vapor is generated. To allow for the vapor produced in one effect to heat the contents of the next effect, a decreasing pressure profile within consecutive effects is necessary. A similar procedure is repeated in each of the remaining effects whereby a portion of the vapor generated in the previous effect is used to convert a portion of the feed entering into the effect into vapor. Within the last effect, all the generated vapors are directed towards pre-heating the feed in a down condenser. However, since the incoming feed is generally not capable of carrying away all the heat required to condense the inputted vapor generated in the last stage, additional cooling water is usually entered into the down condenser, where it is pre-heated and subsequently rejected back to the sea. To recover additional energy in the system, intermediate brine and distillate streams are flashed as they are successively entered into lower pressure chambers.

The source of feed to each effect varies depending on the configuration employed. In the forward feed (FF) MED configuration, all of the feed entering into the system is directed solely to the first effect. No intermediate feed extractions occur as the feed leaves each consecutive preheater, but rather all the feed leaving a particular preheater is lead into the subsequent one. For all the remaining effects, the feed to the effect is comprised of brine exiting from the previous effect. FF is typically advantageous since the brine leaving the highest temperature effect is the least saline; a characteristic that reduces the risk of scaling. The parallel cross (PC) MED configuration, is an alternate configuration. Within this configuration, the feed to each effect is comprised of pre-heated seawater extracted at the outlet of the corresponding feed preheater. Brine exiting each effect is simply flashed to produce additional vapor, without allowing any of the brine to be inserted as feed into any of the subsequent effects. Typically the PC-MED configuration is found to be capable of larger distillate production capabilities compared to FF-MED [28].

MSF largely resembles the MED configuration in its flowsheet with the exception that all the vapors generated in any particular stage are solely directed towards pre-heating the feed in the next unit. As a consequence, no vapors are generated by evaporation in MSF. Interestingly, MSF can be considered to be a more specific and constrained form of MED including flash boxes. The main mode of vapor production in MSF is the process of brine flashing, a process which is possible because of the decreasing pressure profile within consecutive stages. However, some additional vapor does form by flashing condensed distillates. For the same number of repeating units, MSF is characterized by significantly lower recovery ratios (RR), as compared to MED due to the lower thermodynamic efficiency of flashing compared to boiling. MSF has however the advantage that since the top operating temperature can reach up to approximately 110 °C compared to approximately 70 °C in MED, which allows for a larger number of stages in MSF as compared to the number of possible effects in MED. The brine leaving the last stage of the MSF can be returned to the sea as brine blow down, a configuration known as once through MSF (MSF-OT). Alternately, some designers choose to mix a portion of the brine leaving the last stage with the incoming feed to the plant; a configuration known as MSF with brine mixing (MSF-BM).

4. Superstructure proposed for the process

The superstructure was constructed with the constraint that all of the resulting process designs can be physically implemented. The finalized superstructure is represented in Fig. 1. Section 4.1 discusses all the different design options allowed by the process, while Section 4.2 examines how variables can be manipulated to delete different components. Section 4.3 highlights, with the aid of schematics, how the generalized superstructure can be reduced to known configurations. Section 4.4 discusses the main limitations of the current superstructure. Section 4.5 outlines details of the mathematical modeling of different components that could potentially make up the final system. Lastly, Sections 4.6 and 4.7 outline the necessary operation constraints, as well as the choice of optimization variables.

4.1. Design options

Several novel flow patterns are allowed. Fig. 1 provides a schematic illustrating the numerous brine and feed flow routings in the superstructure proposed. For simplicity a total of 12 units is chosen. To maintain a non-convoluted figure, the vapor routings barring the input primary heating steam are not shown in Fig. 1. Fig. 2, however, provides the complete schematic including vapor routings for a sample repeating unit i in the superstructure. A few exemplary design options allowed by the superstructure are also represented in Fig. 2, indicated by the variables (α, λ and ϵ).

The superstructure is built around several discrete/continuous choices:

- The choice of what fraction of the overall feed flow leaving any intermediate feed preheater (FPH) is extracted to be sent to the corresponding MED effect (ϵ) and what fraction is directly sent to the next preheater ($1 - \epsilon$). This is a continuous decision where the condition ($\epsilon = 1$) corresponds to complete extraction, while ($\epsilon = 0$) signals that all feed leaving a preheater is inserted to the next preheater. Any intermediate value corresponds to only a fractional extraction. At the exit of the down-condenser, there is an additional split variable ϵ_1, shown in Fig. 1, which dictates what fraction of total feed is returned to the sea (i.e. serves as cooling water). The fractions ϵ_2 and ϵ_3 then dictate the corresponding fractions that are entered into last effect and fed to the last preheater respectively.
- The choice of what fraction of the total brine leaving a particular brine flash box, is extracted to be fed to the next effect (λ) and what fraction is allowed to be sent to the next flash box in the same flash box line ($1 - \lambda$). This feature allows the model an interesting option of using brine outputted from any effect i as feed to any effect j, where $j > i$.
- The choice of what fraction of the available secondary heating steam (comprised of vapors produced by brine evaporation, brine flashing, and distillate flashing) is sent to the next effect (α) to accomplish brine evaporation, and what fraction is sent to the corresponding feed preheater to achieve feed pre-heating ($1 - \alpha$). In literature, designers often allocate all the vapor formed by brine flashing towards the end of feed pre-heating, and fix all the vapors formed within an effect towards the end of heating contents of the next effect. By combining all the formed vapors, and subsequently choosing a value for α, some of the vapor formed by brine flashing

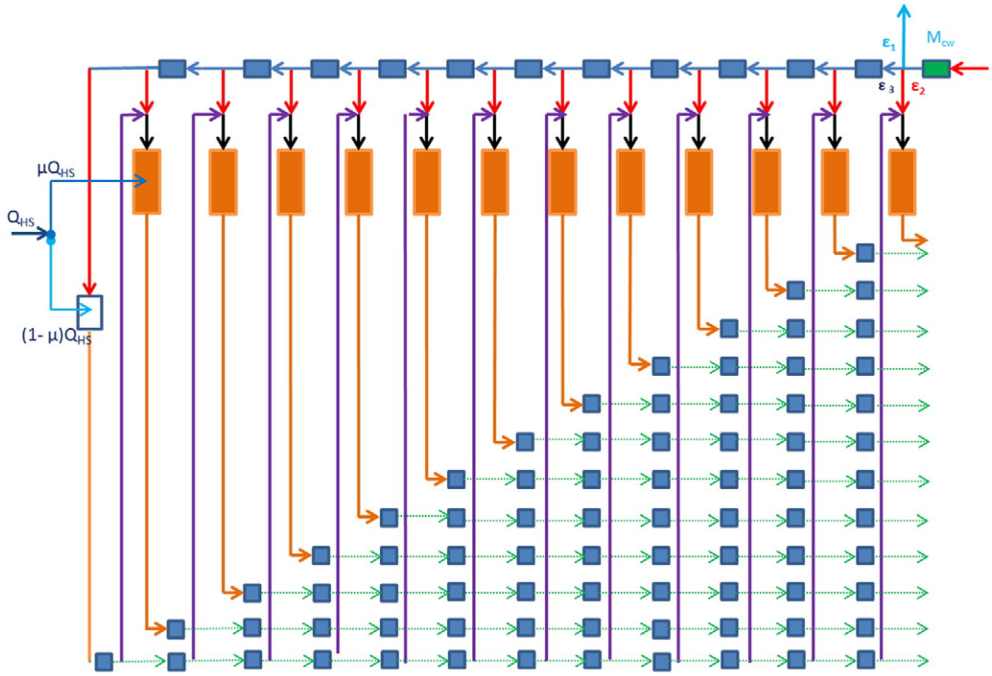

Fig. 1. Generalized superstructure illustrating different brine and feed routings. Without loss of generality, 12 repeating units are shown. Vapor routings are shown in Fig. 2.

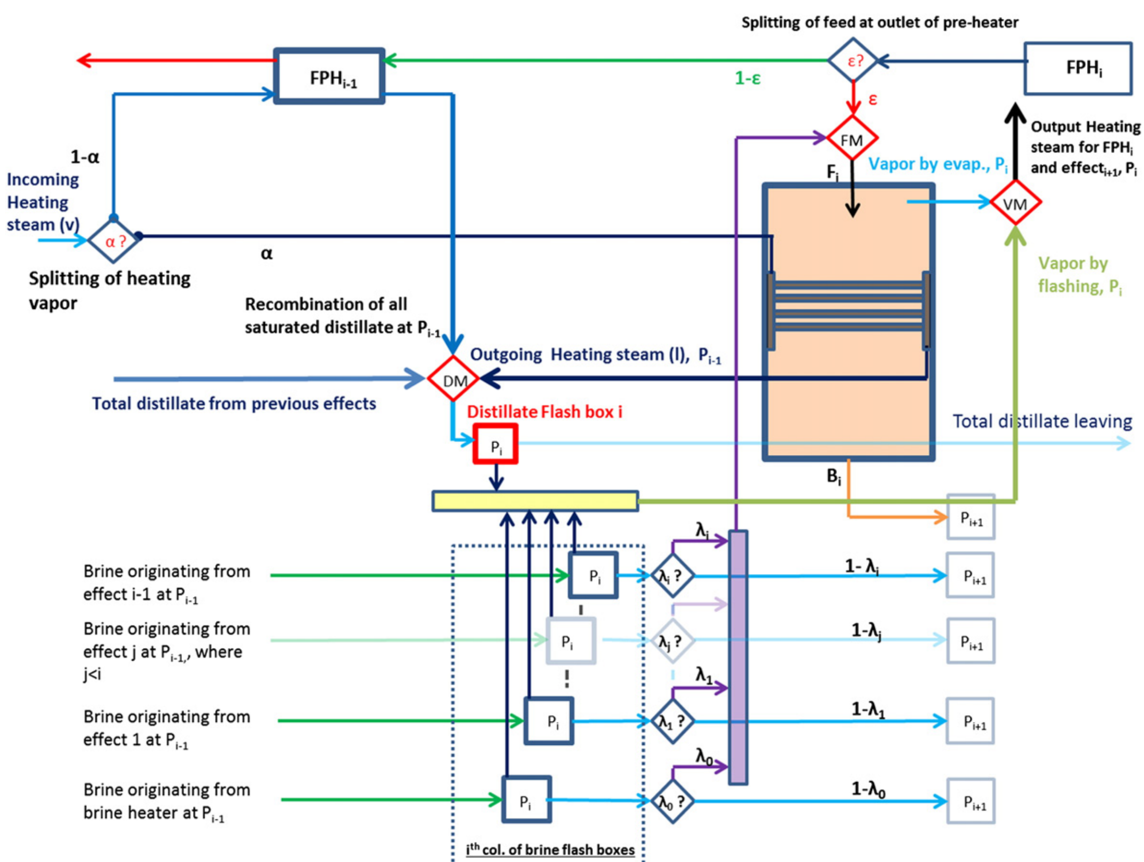

Fig. 2. Representation of the repeating unit i of the proposed superstructure, demonstrating vapor, feed and brine alternate routings.

could be used towards brine evaporation within next effect, while some of the vapor formed by evaporation within an effect could be used towards feed pre-heating in the next unit of superstructure.
- The choice of what fraction of the primary heating steam available is directed towards the 1st MED effect for evaporation (μ) and what remaining fraction is directed towards the brine heater corresponding to the MSF line ($1 - \mu$) is shown in Fig. 1.

For the example of 12 effects, optimization of the superstructure has to ultimately decide on the optimal values for each of the 13 ϵ, 72 λ, 12 α and 1 μ variables. In total these 98 different variables dictate a very large combination of possible hardware components, and combination of possible finalized flowsheets (in excess of 10^{40} structures).

4.2. Post-processing to identify optimal hardware

The general superstructure, made up of N repeating units, is capable of representing a maximum of N effects, N feed preheaters, $N - 1$ distillate flash boxes and a maximum of $N^2/2$ different brine flash boxes. The superstructure is flexible in adapting what subset of allowable components is ultimately used. One interesting and extremely useful feature of the implementation is that components can be deleted without the need to resort to any integer variables which is the traditional method of implementing superstructures as in [27,29,30]. Avoiding the use of integer variables greatly minimizes the relative difficulty of system optimization, which the superstructure will eventually be used for.

Assuming the optimization is complete, a thorough post-processing of the value of the different system variables signals whether a component is included. Deletion of an effect is signaled either by the absence of any incoming feed into the effect, or alternately by the absence of any vapor production by evaporation within the effect. Deletion of a preheater component is indicated by the absence of any heating vapor being directed towards it (i.e., the corresponding $\alpha = 1$), which is synonymous to an absence of any temperature difference as the flow passes through the device; a sign that no heat transfer occurred. For brine and distillate flash boxes, elimination of the hardware is signaled by the absence of an incoming flow into the component. To the end of determining whether a specific brine or feed flow is negligible, cut-off assumptions are enforced. Specifically, any flow representing less than 0.2% of the mass flow rate of incoming feed is neglected. The presumption is that the benefit of this marginal flow to the overall system level performance would likely not justify the inclusion of an additional component once a more thorough economic analysis is conducted.

While the superstructure is capable of representing $N^2/2$ different brine flash boxes, it can be envisioned that capital costs associated with that many separate components would be tremendously high. Fortunately, the number of brine flash boxes can be manually reduced in the post-processing phase through a recursion. A group of brine flash boxes operating at a common pressure can be combined into one equivalent operating flash box operating at the same pressure if all of their outputs are redirected to the same location to mix. This process is repeated until no two differing brine flash boxes operating at the same pressure feed all their output into the same location.

4.3. Representation of conventional configurations

Through an appropriate choice of extraction variables, the superstructure can represent known structures. For illustrative purposes, the process diagrams for the FF-MED (Fig. 7), the PC-MED (Fig. 8), and the OT-MSF (Fig. 9) are figuratively represented, whereby the transparency of the streams and components signals their exclusion. These figures are found in Appendix A. It is worth highlighting that the intermediary heating steams are not shown in the schematics. The procedure, however, is to combine all the vapor streams formed by all the different modes of vapor production to form an overall heating steam, which is subsequently split appropriately among the feed heater and effect.

4.4. Limitations of superstructure

In general, a superstructure represents all the options that the authors perceive to be potentially advantageous. Herein, the superstructure does not allow the option of the backward feed which is considered disadvantageous; the process of redirecting brine outputted from an effect to a higher pressure prior effect. A configuration characterized by backward feed has an increased risk of scaling since the highest temperature effects are also characterized by the highest salinities. Moreover, the brine exiting an effect would have to be pumped from one effect to the next which would significantly increase pumping requirements.

Within the last effect certain options such as the recirculation and mixing of part of the brine blow down with incoming feed are not represented. This is a common procedure in MSF configurations. However, since only 12 units of the superstructure is implemented in this work, the dominant structures are expected to take the form of MED structures, where this option is not common. Nevertheless, it would be interesting to investigate whether such an idea has merit in future versions of the superstructure.

The mathematical model computes most of the important metrics including the RR (defined as the fraction of the feed converted to distillate), the performance ratio and the specific area requirements. An accurate determination of the geometry of the individual components, however, is not computed in this work. As a result, pumping requirements which themselves are heavily dependent on geometry, are not accurately determined.

4.5. Mathematical representation

A detailed description of the mathematical modeling of the different system components which include the effects, preheaters, flash boxes, mixers and splitters is provided in Appendix B. The mathematical modeling is based on mass, species and energy balances around each of the components. Appendix C describes how the heat transfer requirements within the effects and preheater are determined, while Appendix D outlines the main assumptions utilized in this model. Note that the model assumptions correspond essentially to standard models in literature. Such a model is adequate for the aim of this article, i.e., a methodology for structural optimization and identification of interesting potential structures. Substantially improving the model accuracy would result in a significantly more complicated model; this would change little in our methodology but present an optimization problem which is most likely intractable with state-of-the-art optimizers.

Appendix B provides the general equations defining how mixers and splitters operate. It is clear, however, by inspecting Figs. 1 and 2 that numerous mixers and splitters occur within the overall system. Three different instances of mixing occur within any particular superstructure unit, indicated in Fig. 2. A feed mixer (denoted in Fig. 2 as FM) allows the formation of the total feed to an effect by allowing the blending of several brine streams extracted from the appropriate flash boxes with extracted feed exiting from a preheater. A vapor mixer (denoted in Fig. 2 as VM) combines all generated vapor streams produced in a particular unit to form the overall heating to the next unit of the superstructure. Finally, a distillate mixer (denoted in Fig. 2 as DM) merges the condensed heating steam with the combined distillate produced in prior units. The distillate output from DM is fed into an appropriately pressured distillate flash box where it flashes.

Splitters, on the other hand, can be seen to occur at multiple system locations which include the outlet of the down condenser, the outlet of each of the preheaters as well as the outlet of each of the brine flash boxes. A further splitter divides the input heating steam so that a fraction of it can be directed to heat contents of the first effect, while the remainder is directed to the brine heater. Further splitters occur at the outlet of the each of the VMs to segregate the vapor to be used for feed pre-heating from the vapor to be used for evaporation within the appropriate effect.

4.6. Operational constraints

To ensure the feasibility of the finalized structure, several temperature constraints need to be enforced. The constraints include:

1. Saturation temperature of the brine decreases with effect number.
2. The temperature of the heating steam exceeds the temperature of the feed it is used to heat at both the outlet and inlet of each preheater.
3. The saturation temperature of the heating steam is greater than the saturation temperature of the brine within the effect it is designated to heat.
4. The temperature of the feed exiting a preheater is not less than the temperature of the feed entering a preheater.
5. The temperature of the cooling water leaving the down condenser does not exceed the temperature of the vapor generated in the last effect.

Although it is customary to set minimum pinches in heat exchangers, this work avoids doing so. Since one of the objective functions will always include an economic related metric, the optimizer will itself seek a solution where sufficiently large temperature differences between the heating and heated medium are always made available.

4.7. Optimization variables

In all subsequent optimization studies performed using the superstructure, the optimization variables include a subset of the variables to be discussed herein. The first set of optimization variables are the split ratios discussed in Section 4.1, which are considered to be continuous, with possible values ranging from 0 to 1. The other potential optimization variables are the overall feed flow rate to system, the saturation temperature within each of the effects, as well as the temperature profile of the feed at the inlet and outlet of each of the preheaters. A setup where all the aforementioned variables are not preset in any way prior to the optimization will from hereupon be referred to as unconstrained superstructure optimization.

Once the value of all the optimization variables is determined, simple mass and energy balances can be used to determine the flow rates and concentrations of all the brine, feed and distillate streams within the system. The different thermodynamic losses and overall heat transfer coefficients can then computed, which allow the determination of the required sizing of each of the system components.

While optimization of the unconstrained superstructure is always expected to yield the best results, the superstructure can be used in alternative investigations where some of the optimization variables are input into the problem as fixed parameters. For instance, to identify the optimal operation conditions associated with a conventional PC-MED or FF-MED configuration, all the split ratios are specified as parameters to the optimization problem. Further uses of the superstructure will be illustrated in several case studies presented in Section 5.

Table 2
Comparison of minimum SA requirements ($m^2/(kg/s)$) for different locations of seawater extractions; RR = 0.38, $T_{HS_{input}}$ = 70 °C.

	Standard	Mediterranean	Red Sea	Arabian Gulf
T_{sw}	20 °C	26 °C	28 °C	26 °C
X_{sw}	3.5 g/kg	3.8 g/kg	4.1 g/kg	4.5 g/kg
PR = 10	359.2	388.3	413.6	403.8
PR = 10.5	371.0	402.3	428.2	418.7
PR = 11	392.8	429.0	457.6	453.4
PR = 11.25	422.4	467.6	501.1	515.0
PR = 11.5	590.6	667.8	758.2	963.5

5. Case studies involving stand-alone thermal structures

This section intends to highlight the wide capabilities of the superstructure through three illustrative case studies. All the case studies considered herein deal with optimization of standalone thermal configurations. The main intention of the first case study is to illustrate how optimization of the superstructure yields significantly improved configurations relative to the conventional thermal configuration restricted by conventional design specifications. Further, the study shows that even if the choice of plant is restricted to one of the conventional designs, the optimal design is heavily dependent on many factors including distillate production requirements. The second case study, presented in Section 5.4, examines the effect of the temperature and salinity of the incoming feed-water on the resulting optimal structures. The study exhibits the power of the superstructure to quickly identify both the optimal flowsheet and the optimal operational conditions under varying local seawater conditions. Finally, the third case study shows how the effect of certain parameters (e.g. RR) on plant performance could be systematically investigated through a repeated process of varying the value of the parameter in question and repeating the superstructure optimization. Since the superstructure allows the varying of both the hardware and flow patterns between different runs, this study allows designers to better gauge the impact of the parameter in question compared to traditional parametric and optimization studies.

An overview of the problem definition, which includes the objective functions used as well as the mode of optimization, is presented in Section 5.1. The software utilized in this work, coupled with the solution methodology is outlined in Section 5.2.

5.1. Problem definition

The optimization problem considered herein is to determine both the optimal structure and the optimal operating conditions required to produce freshwater at the lowest possible cost. A multi-objective optimization is performed in the three case studies. Specifically, two different objective functions are chosen; one to represent the thermodynamic efficiency and the other to represent the economic costs. Maximizing thermodynamic efficiency is accomplished by maximizing the distillate production on a per unit of heating steam basis, a parameter known as the performance ratio (PR); note that here PR is defined as the mass ratio to stay dimensionless; in industry other units are used as well. Maximizing

Table 1
Comparison of minimum SA requirements ($m^2/(kg/s)$) for different design specifications for PR = 10, 10.5, 11 and 11.25 for T_{sw} = 25 °C, salinity = 4.2 g/kg, RR = 0.41.

Design specification	PR = 10	PR = 10.5	PR = 11	PR = 11.25
Unconstrained superstructure	**389.2**	**403.0**	**427.4**	**469.4**
General FF-MED	**389.8**	**408.5**	468.0	569.4
FF-MED with equal area within effects	395.4	408.9	469.1	582.5
FF-MED with equal temp. diff. between effects	392.1	410.6	468.6	583.4
PC-MED with near equal feed in all effects	431.4	418.9	**438.7**	**485.8**
PC-MED with max. brine salinity at effect exit	418.2	421.7	441.8	488.5

PR can also be thought of in terms of reducing operating costs of the plant, since less heating steam would be required to achieve fixed freshwater production requirements. Minimization of costs is attained through the minimization of the specific heat transfer area requirements (SA) within the system. This is chosen as the preferred metric corresponding to capital costs. Although more detailed cost metrics could have been utilized, these are usually strongly dependent on prices which vary with geographical location and with time. It is useful to note that the methodology could be easily adapted to different relevant metrics. However, this might potentially result in optimization problems which are harder to solve. If in particular the presence of units is penalized, most likely integer variables would need to be introduced.

The aforementioned multi-objective optimization problem is solved by reducing the problem to a series of single objective optimization problems [31,32]. In each step, the PR is set prior to optimization. The optimization problem is reduced to finding the minimum SA required to satisfy the distillate production requirements. This same process is repeated for a series of different PRs. Ultimately, a Pareto frontier is formed which relate the minimum SA requirements for each PR, for wide span of different PRs. Each individual optimization represents a single data point on the Pareto frontier. Note that the approach followed together with the deterministic global optimizers used guarantees the global solution of the optimization problems and thus the Pareto frontier; this cannot be guaranteed using stochastic algorithms such as evolutionary multiobjective optimizers.

5.2. Software and solution methodology

The superstructure was initially implemented using the JACOBIAN software package [33]. JACOBIAN is advantageous since it employs a simultaneous equation solver, which facilitates modeling by allowing the model equations to be inserted in whatever order is most intuitive, without the designer having to worry about the development of cumbersome algorithms to reach solution convergence. The only necessary condition is that the final set of equations is fully determined. The solver then identifies the equations and groups them into fully-determined blocks, which are subsequently solved iteratively to convergence. The accuracy of the generated model was verified by successfully reproducing the results attained by Zak [22], which in turn were validated against literature models.

The verified JACOBIAN model was then converted (using an in-house script) to an equivalent model implemented in General Algebraic Modeling System (GAMS), a system suited for numerical optimization. GAMS was chosen since it is tailored for the optimization of complex, large-scale models and allows for the interface with numerous high-performance solvers [34]. To globally solve the non-linear problem of this study, the Branch-And-Reduce Optimization Navigator (BARON) was used [35,36]. To facilitate model convergence, the generalized reduced gradient algorithm, CONOPT, is used as a local solver to quickly find an initial feasible solution within a few iterations [37,38]. Theoretically, finding a global solution should be independent of the initial guesses. Practically speaking, however, it is found that faster and more probable convergence is attained when good initial guesses are provided. In addition to good initial guesses, it is especially important to have tight lower and upper bounds for each of the system variables; this helps significantly reduce the feasible space the optimizer has to navigate. Finally, to achieve a robust model, the model must be well scaled, with expected values for variables of around 1 (e.g. from 0.01 to 100). For instance, variables such as seawater salinity are preferably expressed as 4 g/kg, as opposed to 40,000 ppm which is often done in literature. Good initial guesses, sufficiently tight bounds of the variables as well as appropriate scaling are all ensured.

The model solution is difficult since the mathematical model involves many variables (more than 1200 variables) and many constraints (1150 equations and inequalities). Attaining good initial guesses for the final optimization model, the step necessary for an efficient solution procedure, was performed in a sequence of steps. The first GAMS optimization is run with zero degrees of freedom which in essence is the equivalent of running a simulation. The attained variable values which are stored in an output file generated by GAMS become the initial guesses for the subsequent optimization. Instead of allowing the system all the proposed degrees of freedom at once which results in very high CPU requirements, the additional degrees of freedom are allowed to the system sequentially, whereby several equations are relaxed at a time. Each time additional degrees of freedom are made available to the system, the optimization is rerun using CONOPT, where the generated output file serves as the initial guesses for the next optimization run where more equations are relaxed. Once good initial guesses are determined, the final optimization is run using the global deterministic NLP solver BARON.

5.3. Case study 1: testing different design specifications

In the literature there are contradicting claims for the optimal thermal structure motivated by different design criteria. Proponents of the FF-MED arrangement have suggested alternative schemes. Some authors suggest that equal heat transfer areas in each of the effects are preferable, as in [39,40]. This specification is projected to result in cost savings associated with buying identical units. Others have suggested a FF-MED scheme characterized by an equal drop in brine saturation temperature between effects [41], so as to minimize the area requirements. Proponents of the PC-MED arrangement propose different preferable conditions. These include fixing the concentration of the brine exiting each effect to the maximum allowable concentration; an arrangement intended to maximize overall distillate production through maximizing RR within each effect [28]. Others specify near equal feed to each effect [5].

While each of the configurations has perceived advantages, this study compares the usefulness of each of the design criteria by comparing the performance of the optimal structure that satisfies the design requirements to the optimal structure attained by optimizing the superstructure with all its degrees of freedom. In each case, the design criteria are enforced by additional equations over and above the ones representing the model of the most general superstructure.

To ensure fair comparison among structures, the RR that all structures must satisfy is set. Since the feed entering into the effects must be pre-treated, setting a common RR ensures comparable pretreatment and pumping costs on a per unit of distillate basis. The optimization problem is then run according to described methods in Sections 5.1 and 5.2. Table 1 shows the comparison of the results attained under different specifications.

The results, as indicated in Table 1, confirm that for any particular distillate product requirement, the configuration arising from the superstructure optimization requires lower SA requirements than the optimal configuration arising from any of the proposed design specifications. This is expected given the additional degrees of freedom available to the unconstrained optimization, but nevertheless confirms that none of the already proposed structures are already optimal.

Table 1 indicates that the optimal general FF-MED (i.e., one without imposed constraints regarding equal areas or equal temperature differences) is a desirable structure for low distillate production requirements ($PR = 10$, and $PR = 10.5$) since the SA requirements closely match those required by optimal structures arising from the unconstrained optimization. At higher distillate production requirements ($PR = 11$, and $PR = 11.25$), however, implementation of the FF-MED is not encouraged since the SA requirements exceed those of the superstructure by up to 21%. Table 1 further suggests that it is important to revise traditional design specifications such as imposing equal areas and equal temperature differences, which are shown to require slightly larger SA requirements (2% higher for PR = 11.25) than the general FF-MED configuration. Although equal areas within the effects may be more practical from an implementation standpoint, this practicality comes at the expense of extra area requirements; a trade-off that must be looked into in more depth by designers.

Table 1 indicates that the PC-MED with near equal feed entering each effect is optimal. The near equal feed constraint is imposed by dictating that none of 12 effects receives less than 1/15 of the total feed entering into the configuration. Still, results suggest that alternate structures motivated by the superstructure require significantly lower SA requirements at high PR requirements (3.5% reduction in SA requirements for PR = 11.5).

5.4. Case study 2: identifying optimal structures depending on location

Desalination plants extract seawater from varying bodies of water including the Mediterranean, the Red Sea and the Arabian Gulf, each of which is characterized by a different temperature and concentration. While experience in one area of the world could provide invaluable lessons applicable in other regions, the need to optimize configurations taking into account local conditions is irreplaceable. This case study identifies the optimal structure depending on the origin of seawater extraction for different PR requirements. For the sake of this study, constant nominal conditions are assumed according to [24]. Typically however, these conditions vary throughout the year, and ideally it would be best to optimize the structure taking into account the year round varying conditions. The superstructure in this case study is ensured to satisfy the form of a 12 effect MED, by adjusting the lower bounds of vapor production within each of the effects to an appropriate positive value.

Results of this study, indicated in Table 2, suggest that for 12 effect MED structures, feed streams characterized by lower temperatures and concentrations require lower SA requirements. This may seem counter-intuitive since most of MED plants are installed in Saudi Arabia and the United Arab Emirates; countries which are mostly in contact with the Arabian Gulf. Moreover, countries with the seemingly favorable standard conditions have not exhibited significant installed MED capacities in recent times. Ultimately, however, the likelihood of implementation of a structure is heavily influenced by the local fuel costs which are low in the Middle East, and the relative competitiveness of RO; a technology characterized by deteriorated performance at elevated salinity values. It is confirmed that the optimal configurations differ in the proposed flowsheet depending on the environmental conditions.

5.5. Case study 3: investigating influence of RR

For a fixed distillate production requirement, a higher RR results in lower overall flow of feed to the plant; and consequently both lower pretreatment costs and pumping requirements. Generally, whenever the maximum distillate production is desirable, the RR is maximized by designers insofar as scaling can be avoided. However, while increasing RR might increase distillate production, it has the disadvantages of increase SA requirements by increasing boiling point elevation losses. This study seeks to quantify the reduction in SA requirements (reducing capital costs) attained by reducing the RR constraint (increasing operating costs).

Fig. 3 shows the results attained through this analysis for four differing PR requirements. It can be clearly seen that for a fixed PR, allowing for a decrease in required RR can result in significant decreases in SA requirements. This observation suggests that the ensuing reduction in capital costs might justify the additional operating costs the operators must tolerate. Ultimately designers must weigh differing factors such as the cost of pre-treating the incoming feed (dependent on feed concentration), and the cost of different heat transfer areas before deciding which combination of optimal (PR, SA, RR) is preferable.

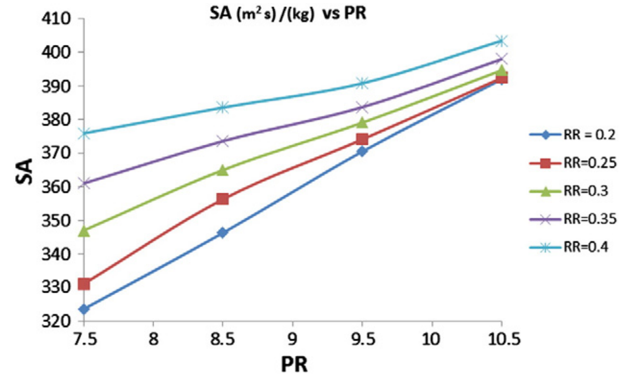

Fig. 3. Comparison of minimum SA requirements ($m^2/(kg/s)$) for different recovery ratios for 4 distillate production amounts.

5.6. Examples of optimal structures

While Section 5 illustrates that some non-conventional structures exhibit improved performance, this section presents the flow diagrams for some of prevalent optimal structures. The optimal structures for PR = 8.75 (Fig. 4), PR = 10.25 (Fig. 5) and PR = 11 (Fig. 6), under the assumption of RR = 40%, are all shown. The figures depict the optimal flow rates of all the different brine and feed streams, under the assumption of a 10 kg/s flow rate of input heating steam (not shown in the figure). Note that the absence of a particular preheater signals that all the vapors produced in the previous superstructure unit are sent in whole to the next effect.

It can be seen that the presented structures are indeed non-standard, and do not follow any particular pattern with respect to how flows are directed. For this reason, it is difficult to clearly categorize these structures, although some of the structures do exhibit FF-MED and PC-MED like characteristics.

For instance, the optimal PR = 8.75 structure is similar to the FF-MED in the sense that no intermediate extractions occur. Moreover, all the brine outputted from the effects is completely redirected to the next effect. The optimal PR = 10.25 structure is interesting in that it resembles two FF-MED configurations connected in series. More precisely, the configuration is made up of a 7 effect FF-MED structure connected to a 5 effect FF-MED. The feed entering the 7 effect FF-MED is pre-heated by the preheaters corresponding to the 5 effect FF-MED. Moreover, as indicated by Fig. 5, the concentrated brine leaving the 7th effect is not inserted into any of subsequent effects, but rather flashed in a series of flash boxes to recover further energy from the brine. This action allows the 5 effect FF-MED to maintain lower outlet salinity brine at exit of its effects, which subsequently reduce boiling point elevation losses and thus reduce area requirements.

Compared to the lower PR structures, the optimal PR = 11 structure allows more frequent intermediate feed extractions from the main feed pre-heating line. The result is a lower amount of feed entering into the initial effects. The resulting reduction in sensible heating requirements allows for more vapor generation in the early effects, which ultimately increases the total distillate that can be formed in the structure. It is worthy noting the unconventional brine routing in the structure. For instance, the brine outputted in the 4th effect for instance is fed into the 10th effect, while the brine outputted from the 10th effect is allowed to by-pass all of the later effects.

A cursory look at the structure shows that optimization must be employed to obtain thermoeconomically favorable structures. For

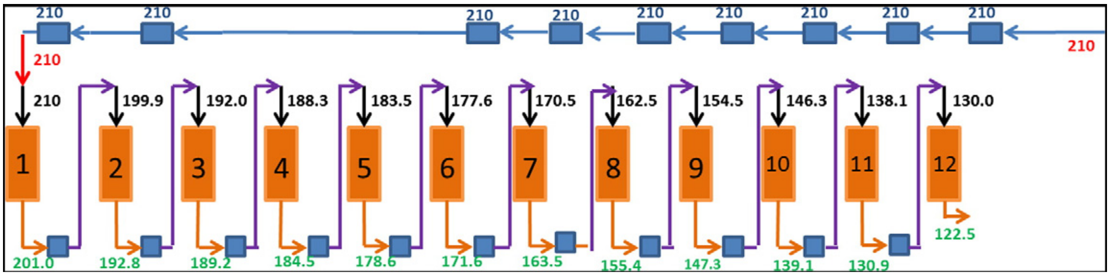

Fig. 4. Optimized configuration for PR = 8.75.

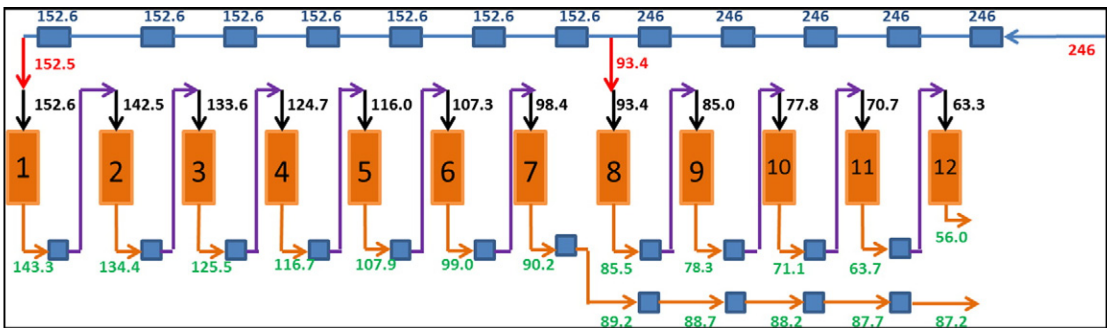

Fig. 5. Optimized configuration for PR = 10.25.

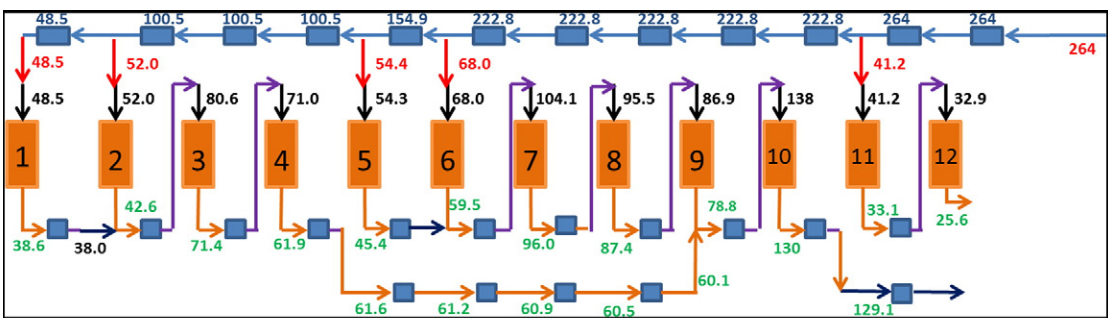

Fig. 6. Optimized configuration for PR = 11.

instance, a designer with the knowledge of the optimal structures corresponding to PR = 8.75 and PR = 10.25 would still not be able to accurately predict the optimal flowsheet for a structure corresponding to PR = 9.5.

6. Conclusions

The capability of the developed superstructure in identifying improved stand-alone thermal structures has been demonstrated simultaneously allowing for both MSF and MED stages. It is important, however, to stress that the enabling features of the superstructure are not restricted to only the illustrative case studies presented earlier in this paper. Given the flexible methodology applied to modeling the superstructure, it can be easily modified for alternate useful studies. One such possible study is to assess the merits and trade-offs associated with integrating thermal desalination plants with thermal vapor compression units through a steam ejector. Another study of interest is to investigate if subcooling the inputted heat steam improves plant performance; the contrary claim has been made in the literature. Yet another study could assess alternate optimal configurations integrating both thermal and membrane technologies as part of hybrid thermal-membrane scheme.

Further, the superstructure can assist in the production of optimal operation for fixed design. If a plant is already in use (i.e., component set and size of components are already specified), the superstructure could be easily adjusted to optimize operating conditions.

Another useful application that the superstructure lends to designers is testing the sensitivity of configurations to relaxed technological constraints. For instance, if the top brine temperature is increased to 120 °C instead of 70 °C through improved anti-scalants, optimization of the superstructure can help identify how much improvement such a development would yield and would also inform the designers of the predicted flow patterns under the more favorable conditions. This sort of work, repeated for different possible constraints, can help identify which of the technological constraints are most limiting, a process which can help optimally allocate funding for future R&D projects pertaining to thermal desalination. Mitsos et al. [42] utilize a similar approach for micropower generation and demonstrate the importance of limits of operating temperature and performance of components.

Future work pertaining to modeling includes the implementation of more accurate seawater properties, including the introduction of a latent heat of evaporation/condensation of water that is temperature dependent as is done in [43]. Moreover, the effect of the number of repeating of superstructure units must be studied beyond the assumed 12 repeating units. For instance, approximately 40 stages are needed in order for MSF structures to realistically compete with MED structures in terms of distillate production. Moreover, the additional options of brine re-circulation and brine mixing can be afforded to the last unit within the superstructure, which enhances possibility of identifying improved structures. These more detailed models can be used either directly in superstructure optimization, albeit making the optimization problem substantially harder, or they can be used to analyze the interesting unconventional structures identified using the simpler models.

Nomenclature

Variables	Name of variable	Units
T	Temperature	K
X	Salinity	g/kg
N	Flow variable	kg/s
F	Feed to an effect	kg/s
HS	Heating steam to a superstructure unit	kg/s
V	Saturated vapor	
D	Distillate (saturated liquid)	
B	Brine exiting an effect	kg/s
Q	Rate of heat transfer	kJ/s
L	Latent heat of evaporation/condensation	kJ/kg
c_p	specific heat capacity at constant pressure	kJ/(kg K)
Subscript		
in	Input to a component	

(*continued*)

Variables	Name of variable	Units
out	Output from a component	
sat	Corresponding to saturation conditions of a component	
i	Component number	
Superscript		
BE	Brine evaporation within effect	
BF	Brine flashing within brine flash box	
DF	Distillate flashing within distillate flash box	
Abbreviations		
FPH	Feed preheater	
EFF	Effect	
BFB	Brine flash box	
DFB	Distillate flash box	
BPH	Brine preheater	
RO	Reverse osmosis	
NF	Nano filtration	
MSF	Multi-stage flash distillation	
MED	Multi-effect distillation	
Parameters	Name of variable	Units
PR	Performance ratio	Dimensionless
RR	Recovery ratio	Dimensionless
SA	Specific heat transfer area requirements	$\frac{kg\ s}{m^2}$

Acknowledgments

The authors would like to thank the King Fahd University of Petroleum and Minerals in Dhahran, Saudi Arabia, for funding this work through the Center for Clean Water and Clean Energy at MIT and KFUPM under project number R13-CW-10. We would like to also thank our colleagues at MIT and KFUPM for useful discussions, in particular Gina M. Zak and Prof. John H. Lienhard V.

Appendix A. Conventional configuration schematics

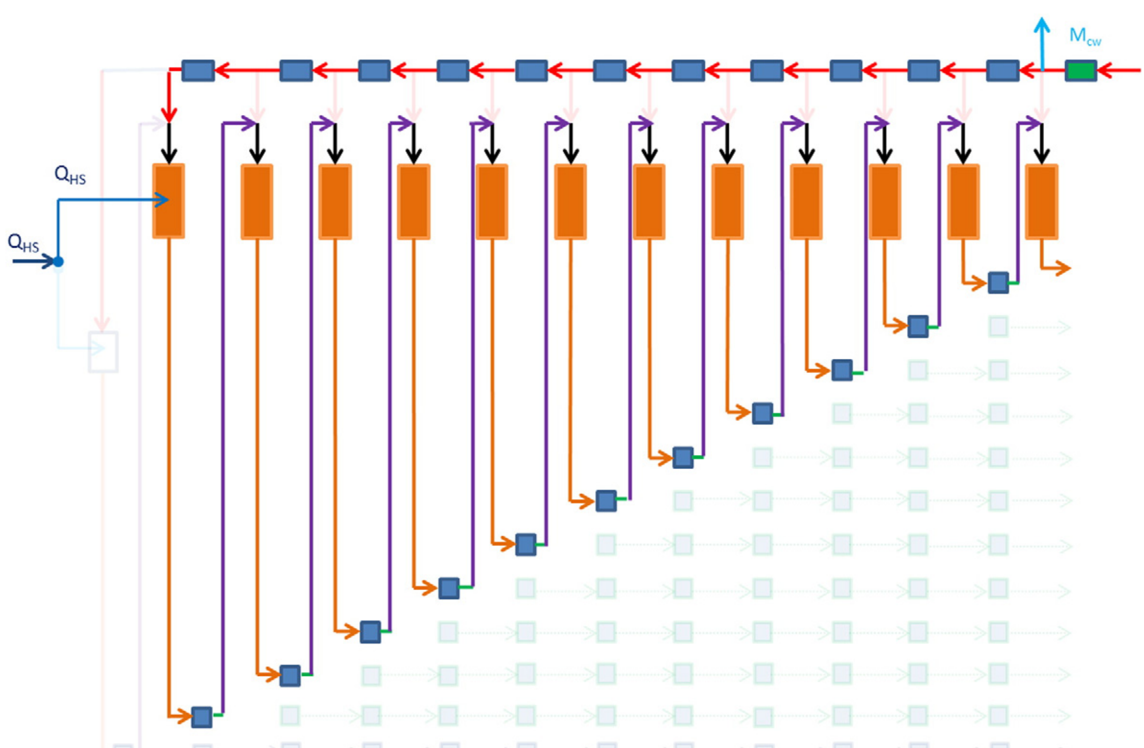

Fig. 7. A 12 effect forward feed (FF) MED, from a simplified superstructure (brine and feed streams only).

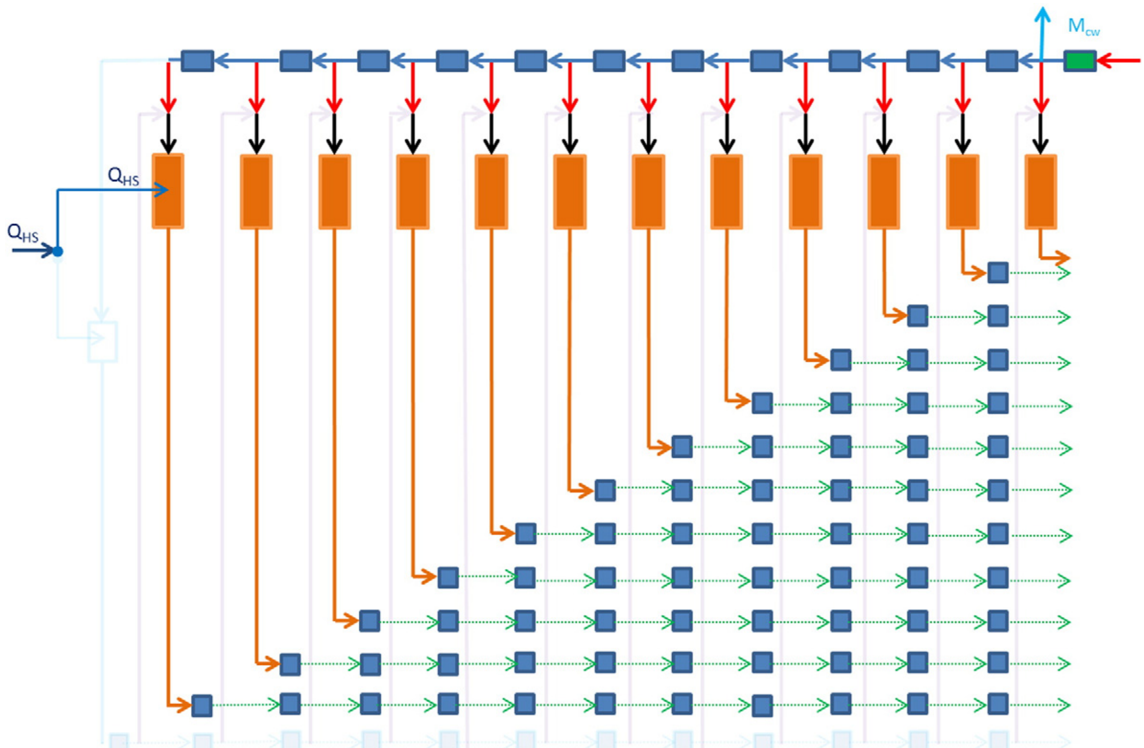

Fig. 8. A 12 effect parallel cross (PC) MED, from a simplified superstructure (brine and feed streams only). Brine flash boxes can be recursively removed to simplify to traditional PC MED.

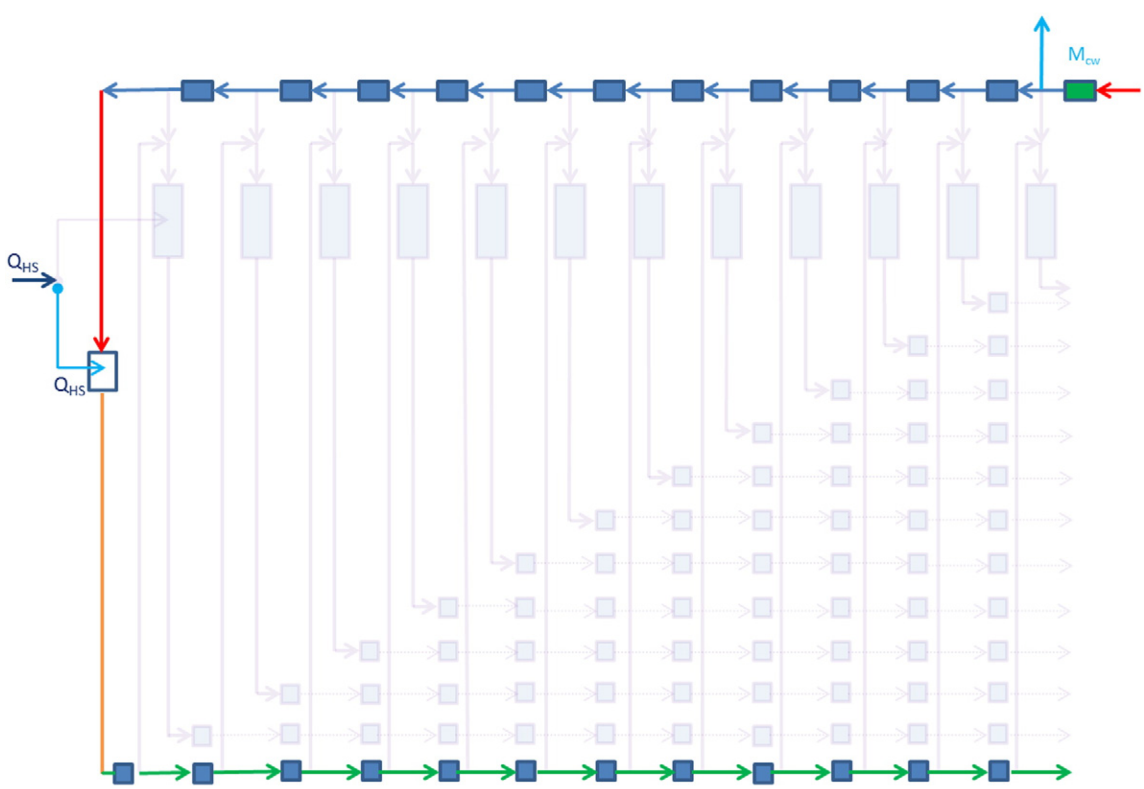

Fig. 9. A 12 stage once through MSF, from a simplified superstructure (brine and feed streams only). Vapor generated in flash boxes is used to pre-heat the feed.

Appendix B. Mathematical model

Mixer

Mixers have one output stream, but multiple input streams. Assuming m different incoming streams each characterized by an incoming mass flow rate N_{in_j}, the mass flow rate of the outputted stream N_{out} can be computed according to the relation:

$$N_{out} = \sum_{j=1}^{m} N_{in_j}. \tag{1}$$

For the mixers dealing exclusively with liquid streams, the model assumptions of incompressible liquid streams and composition-independent enthalpies allow the energy balance to be simplified to:

$$T_{out} = \frac{\sum_{j=1}^{m} N_{in_j} T_{in_j}}{N_{out}}. \tag{2}$$

Moreover, when the composition of the different inlet streams is not identical, the salinity (X) of outlet stream can be computed from a species conservation balance as indicated below:

$$X_{out} = \frac{\sum_{j=1}^{m} N_{in_j} X_{in_j}}{N_{out}}. \tag{3}$$

This work enforces that only saturated vapor streams of the same pressure can mix. For this reason, in the case of vapor mixers, the outlet stream is assumed to always be at the same temperature as the inlet streams.

Splitter

Splitters have one incoming stream, which is subsequently divided into 2 or more streams. Assuming an incoming stream N_{in} and m differing outgoing streams N_{out_j}, splitters are governed by general mass conservation equations as described below:

$$N_{in} = \sum_{j=1}^{m} N_{out_j}. \tag{4}$$

Assuming each outgoing stream is composed of a fraction β_j of original flow, any outgoing stream j can be expressed by relation below:

$$N_{out_j} = \beta_j N_{in} \quad \text{for } j = 1, 2, \ldots, i \tag{5}$$

where:

$$\sum_{j=1}^{i} \beta_j = 1. \tag{6}$$

MED effect

In MED effects, the mode of vapor production is brine evaporation, signaled by the superscript 'be'. In addition to the heat required to evaporate part of the brine, heat is also necessary to first sensibly heat the feed entering into an effect to the saturation temperature corresponding to the effect. Given a specified amount of heat entering into an effect i (Q_{eff_i}), the amount of formed vapor (V^{be}) that can be formed is determined according to the energy balance in Eq. (7).

$$Q_{eff_i} = F_i c_p \left(T_{sat_{eff_i}} - T_{feed_i}\right) + V^{be} L \tag{7}$$

Brine flashing box

In situations where saturated brine $B_{bfb_{in}}$ is entered into a lower pressure brine flash box, the vapor generated by brine flashing (V^{bf}) can be found as:

$$V^{bf} = \frac{B_{bfb_{in}} c_p \left(T_{sat_{in}} - T_{sat_{bfb}}\right)}{L}. \tag{8}$$

Subsequently, the amount of brine outputted from the flash box $(B_{bfb_{out}})$ and its corresponding salinity $(X_{bfb_{out}})$ are determined by a mass balance (Eq. (9)) and a salt balance (Eq. (10)) respectively.

$$B_{bfb_{out}} = B_{bfb_{in}} - V^{bf} \tag{9}$$

$$X_{bfb_{out}} = \frac{B_{bfb_{in}} X_{bfb_{in}}}{B_{bfb_{out}}} \tag{10}$$

The subscript 'bfb' refers to the brine flash box, while the superscript 'bf' refers to mode of vapor production, which corresponds to brine flashing.

Note: The brine flash boxes are chosen to operate at a similar pressure to that of the subsequent effect. This choice allows for the generated vapors to exit at similar pressures to the vapors generated within the effects, which allows for their mixing.

Distillate flashing box

Additional vapor is generated when saturated distillate at temperature $T_{sat_{in}}$ is flashed in a lower pressure box operating at $P_{sat_{dfb}}$. This amount is found according to Eq. (11).

$$V^{df} = \frac{D_{dfb_{in}} c_p \left(T_{sat_{in}} - T_{sat_{dfb}}\right)}{L} \tag{11}$$

The subscript 'dfb' refers to a distillate flash box component while the superscript 'df' refers to distillate flashing.

Preheater

In any particular feed preheater (FPH), a certain portion of heating steam condenses to provide the heat required to pre-heat the incoming feed. Assuming a specified amount of heat transfer Q_{FPH_i} is transferred to the incoming feed flow, the temperature of the feed at the outlet of the preheater can be determined according to Eq. (12) below:

$$Q_{FPH_i} = F_{FPH_i} c_p \left(T_{FPH_{out}} - T_{FPH_{in}}\right). \tag{12}$$

Main brine heater

Essentially also a feed preheater, the function of the main brine heater (MBH) function is to sufficiently heat the incoming feed such that the temperature of the outgoing feed exceeds the saturation temperature corresponding to the brine flash box into which the stream will be entered. This is necessary condition to induce brine flashing, the main mode of production within MSF configurations.

Assuming a total heat transfer of Q_{MBH} is transferred to the main brine heater, the temperature at the outlet of the device is determined according the energy balance in Eq. (13).

$$Q_{MBH} = (F_{MBH})\left(c_p\right)\left(T_{MBH_{out}} - T_{MBH_{in}}\right) \tag{13}$$

Down condenser

The down condenser (dc) is responsible for condensing the vapors generated in the last unit of the structure. This heat is carried away by seawater flowing through the down condenser F_{dc}, which is composed of both cooling water and total feed to rest of the thermal system. As such the amount of heat transfer can be expressed as:

$$Q_{dc} = HS_N L = F_{dc} c_p \left(T_{dc_{out}} - T_{sw}\right). \quad (14)$$

Appendix C. Heat transfer design equations

Design equations to compute the required heat transfer areas within the effects, the preheaters, the down-condenser and the brine heater are developed in this appendix. The heat exchanger areas are assumed to be just large enough condense the heating vapor incoming into the component.

Within the effects, the required heat transfer area A_{eff} is dependent on the overall heat transfer coefficient U_{eff} (herein not accounting for fouling) and the thermal temperature gradient and is computed as:

$$A_{eff_i} = \frac{Q_{eff_i}}{U_{eff_i} \Delta T_{eff_i}}. \quad (15)$$

The thermal gradient ΔT_{eff} within an effect is described by:

$$\Delta T_{eff_i} = Tv_{i-1} - T_{eff_i}. \quad (16)$$

The following relation gives the heat transfer area in the preheaters:

$$A_{FPH_i} = \frac{Q_{FPH_i}}{U_{FPH_i} LMTD_{FPH_i}} \quad (17)$$

where the log mean temperature difference in a preheater ($LMTD_{FPH}$) is calculated as:

$$LMTD_{FPH_i} = \frac{\left(Tv_i - T_{FPH_{i_{out}}}\right) - \left(Tv_i - T_{FPH_{i_{in}}}\right)}{Ln \frac{\left(Tv_i - T_{FPH_{i_{out}}}\right)}{\left(Tv_i - T_{FPH_{i_{in}}}\right)}} = \frac{\left(T_{FPH_{i_{in}}} - T_{FPH_{i_{out}}}\right)}{Ln \frac{\left(Tv_i - T_{FPH_{i_{out}}}\right)}{\left(Tv_i - T_{FPH_{i_{in}}}\right)}}. \quad (18)$$

Similarly, the area requirements within the down-condenser can be computed as:

$$A_{dc} = \frac{Q_{dc}}{U_{dc} LMTD_{dc}} \quad (19)$$

where:

$$LMTD_{dc} = \frac{\left(T_{dc_{out}} - T_{sw}\right)}{Ln \frac{(Tv_N - T_{sw})}{(Tv_N - T_{dc_{out}})}}. \quad (20)$$

In the main brine heater, the requirements are determined as:

$$A_{MBH} = \frac{Q_{MBH}}{U_{MBH} LMTD_{MBH}} \quad (21)$$

where LMTD across the main brine heater is found as a function of the temperature of input heating steam $\left(T_{HS_0}\right)$, as:

$$LMTD_{MBH} = \frac{\left(T_{MBH_{out}} - T_{MBH_{in}}\right)}{Ln \frac{\left(T_{HS_0} - T_{MBH_{in}}\right)}{\left(T_{HS_0} - T_{MBH_{out}}\right)}}. \quad (22)$$

Appendix D. Model assumptions

Thermodynamic assumptions

Given the narrow temperature range within which thermal desalination plants operate, several engineering approximations are justified. First, all liquid streams are considered incompressible. Moreover, a representative value of 4 kJ/kg K is assumed for the seawater specific heat at constant pressure (c_p), which is assumed to be independent of temperature and salinity. Similarly, a constant enthalpy of evaporation of 2333 kJ/kg is assumed. Non-equilibrium allowance is assumed negligible [43,44], while the boiling point elevation (BPE), which determines the variation in the saturation temperature of the brine and formed vapors due to their differing compositions, is computed according to accurate correlations developed by by Sharqawy et al. [45]. These correlations are assumed to be dependent on both the composition and temperature of the saturated brine.

Further engineering assumptions

Several standard assumptions are used to derive the mathematical model. These include:

- Steady state operation.
- Negligible heat losses to the environment.
- Negligible pressure drops across the demister, the connecting lines and during condensation.
- Salt-free distillate (i.e., zero salinity).
- Negligible effect of non-condensable gases on system operation.
- Temperature-dependent overall heat transfer coefficients in both the effects and the preheaters computed according to [41].
- To minimize the risk of scaling, the top brine temperature within effects is upper bounded at 70 °C, while the maximum allowable salinity is upper bounded at 72,000 ppm.

References

[1] Q. Schiermeier, Water: purification with a pinch of salt, Nature 452 (2008) 260.
[2] D. Zhao, J. Xue, S. Li, H. Sun, Q. Zhang, Theoretical analyses of thermal and economical aspects of multi-effect distillation dealing with high-salinity wastewater, Desalination 273 (2011) 292–298.
[3] H.T. El-Dessouky, I. Alatiqi, S. Bingulac, H.M. Ettouney, Steady-state analysis of the multi-effect evaporation desalination process, Chem. Eng. Technol. 21 (1998) 15–29.
[4] P.K. Sen, P.V. Sen, A. Mudgal, S.N. Singh, A small scale multi-effect distillation (MED) unit for rural micro enterprises part II — parametric studies and performance analysis, Desalination 279 (2011) 27–37.
[5] F. Mandani, H. El-Dessouky, H.M. Ettouney, Performance of parallel feed multiple effect evaporation system for seawater desalination, Appl. Therm. Eng. 20 (2000) 1679–1706.
[6] A. Jernqvist, M. Jernqvist, G. Aly, Simulation of thermal desalination processes, Desalination 134 (2001) 187–193.
[7] Y.M. El-Sayed, Design desalination systems for higher productivity, Desalination 134 (2001) 129–158.
[8] S.E. Shakib, M. Amidpour, C. Aghanajafi, A new approach for process optimization of ME-TVC desalination system, Desalin. Water Treat. 37 (2012) 84–96.
[9] H. Sayyaadi, A. Saffari, Thermoeconomic optimization of multi effect distillation desalination systems, Appl. Energy 87 (2010) 1122–1133.
[10] C. Sommariva, D. Pinciroli, E. Sciubba, N. Lior, Innovative configuration for multi stage flash desalination plant, IDA Proceedings, San Diego, I:16, 1999.
[11] S.F. Mussati, P.A. Aguirre, N.J. Scenna, Novel configuration for a multistage flash-mixer desalination system, Ind. Eng. Chem. Res. 42 (2003) 4828–4839.
[12] E. Cardona, S. Culotta, A. Piacentino, Energy saving with MSF-RO series desalination plants, Desalination 153 (2003) 167–171.
[13] A.M. Helal, Hybridization — a new trend in desalination, Desalin. Water Treat. 3 (2009) 120–135.
[14] L. Awerbuch, V. van der Mast, R. Soo-Hoo, Hybrid desalting systems — a new alternative, Desalination 64 (1987) 51–63.
[15] O.A. Hamed, Overview of hybrid desalination systems — current status and future prospects, Desalination 186 (2005) 207–214.
[16] E. El Sayed, S. Ebrahim, A. Al-Saffar, M. Abdel Jawad, Pilot study of MSF/RO hybrid systems, Desalination 120 (1998) 121–128.
[17] M.G. Marcovecchio, S.F. Mussati, N.J. Scenna, P.A. Aguirre, Global optimal synthesis of integrated hybrid desalination plants, Comput. Aided Chem. Eng. 26 (2009) 573–578.

[18] A. Messineo, F. Marchese, Performance evaluation of hybrid RO/MEE systems powered by a WTE plant, Desalination 229 (2008) 82–93.
[19] H. Sayyaadi, A. Saffari, A. Mahmoodian, Various approaches in optimization of multi effect distillation desalination systems using a hybrid meta-heuristic optimization tool, Desalination 254 (2010) 138–148.
[20] H. Choi, T. Lee, Y. Kim, S. Song, Performance improvement of multiple-effect distiller with thermal vapor compression system by exergy analysis, Desalination 182 (2005) 239–249.
[21] L.T. Biegler, I.E. Grossmann, A.W. Wasterberg, Systematic Methods for Chemical Process Design, Prentice Hall, New York, 1997.
[22] G.M. Zak, Thermal Desalination: Structural Optimization and Integration in Clean Power and Water, (Master's thesis) MIT, 2012.
[23] K.M. Sassi, I.M. Mujtaba, Effective design of reverse osmosis based desalination process considering wide range of salinity and seawater technology, Desalination 306 (2012) 8–16.
[24] M. Skiborowski, A. Mhamdi, K. Kraemer, W. Marquardt, Model-based structural optimization of seawater desalination plants, Desalination 292 (2012) 30–44.
[25] S.F. Mussati, P.A. Aguirre, N.J. Scenna, Improving the efficiency of the MSF once through (MSF-OT) and MSF-mixer (MSF-M) evaporators, Desalination 166 (2004) 141–151.
[26] S.F. Mussati, P.A. Aguirre, N.J. Scenna, Superstructure of alternative configurations of the multistage flash desalination process, Ind. Eng. Chem. Res. 45 (2006) 7190–7203.
[27] S.F. Mussati, P.A. Aguirre, N.J. Scenna, Optimization of alternative structures of integrated power and desalination plants, Desalination 182 (2005) 123–129.
[28] G.M. Zak, A. Mitsos, Hybrid thermal — thermal desalination structures, Desalination (2012) 1–15, http://dx.doi.org/10.1080/19443994.2013.803769.
[29] S.F. Mussati, P.A. Aguirre, N.J. Scennas, A rigorous, mixed-integer, nonlinear programming model (MINLP) for synthesis and optimal operation of cogeneration seawater desalination plants, Desalination 166 (2004) 339–345.
[30] E.M. Ferreira, A.P. Balestieri, M.A. Zanardi, Optimization analysis of dual-purpose systems, Desalination 250 (3) (2010) 936–944.
[31] A. Pertsinidis, I.E. Grossmann, G.J. McRae, Parametric optimization of MILP programs and a framework for the parametric optimization of MINLPs, Comput. Chem. Eng. 22 (Suppl.) (1998) S205–S212.
[32] D. Li, J.B. Yang, M.P. Biswal, Quantitative parametric connections between methods for generating noninferior solutions in multiobjective optimization, Eur. J. Oper. Res. 117 (1999) 84–99.
[33] Jacobian modeling and optimization software, Numer. Technol. (2009).
[34] A. Brooke, D. Kendrick, A. Meeraus, GAMS: A User's Guide, The Scientific Press, 1988.
[35] M. Tawarmalani, N.V. Sahinidis, A polyhedral branch-and-cut approach to global optimization, Math. Program. 103 (2) (2005) 225–249.
[36] N.V. Sahinidis, BARON: a general purpose global optimization software package, J. Glob. Optim. 8 (2) (1996) 201–205.
[37] A. Drud, CONOPT — a GRG code for large sparse dynamic nonlinear optimization problems, Math. Program. 31 (2) (1985) 153–191.
[38] A. Drud, CONOPT — a large-scale GRG code, ORSA J. Comput. 6 (1992) 207–216.
[39] H.T. El-Dessouky, H.M. Ettouney, Fundamentals of Salt Water Desalination, Elsevier, 2002.
[40] H.T. El-Dessouky, G. Assassa, Computer simulation of the horizontal falling film desalination plant, Desalination 55 (1985) 119–138.
[41] H. El-Dessouky, I. Alatiqi, S. Bingulac, H. Ettouney, Steady-state analysis of the multiple effect evaporation desalination process, Chem. Eng. Technol. 21 (1998) 437–451.
[42] A. Mitsos, B. Chachuat, P.I. Barton, Methodology for the design of man-portable power generation devices, Ind. Eng. Chem. Res. 46 (22) (2007) 7164–7176.
[43] K.H. Mistry, M.A. Antar, J.H. Lienhard V, An improved model for multiple effect distillation, Desalin. Water Treat. 51 (2013) 807–821.
[44] P. Druetta, P. Aguirre, S. Mussati, Optimization of multi-effect evaporation desalination plants, Desalination 311 (2013) 1–15.
[45] M.H. Sharqawy, J.H. Lienhard V, S.M. Zubair, Thermophysical properties of seawater: a review of existing correlations and data, Desalin. Water Treat. 16 (2010) 354–380.